Journal of ELECTRONIC MATERIALS, Vol. 49, No. 8, 2020
https://doi.org/10.1007/s11664-020-08003-2

TOPICAL COLLECTION: 19TH INTERNATIONAL CONFERENCE ON II-VI COMPOUNDS

Design of a Surface Plasmon Resonance-Enhanced ZnO Ultraviolet Photodetector Based on a Sub-wavelength Metal Grating Covered with a High-Refractive-Index Medium

JI YU,[1] HAI-JIAO MEN,[1] JIAN-WEI ZHANG,[2] XIANG-WEI ZHANG,[3] and NING TIAN[1,4]

1.—College of Physics Science and Technology, Shenyang Normal University, Shenyang 110034, People's Republic of China. 2.—State Key Laboratory of Luminescence and Applications, Changchun Institute of Optics, Fine Mechanics and Physics, Chinese Academy of Sciences, Changchun 130033, People's Republic of China. 3.—College of Photoelectric Engineering, Xi'an Technological University, Xi'an 710021, People's Republic of China. 4.—e-mail: tiann08@163.com

To realize a surface plasmon resonance-enhanced zinc oxide (ZnO) ultraviolet photodetector based on a sub-wavelength metal grating, we take advantage of the sensitivity of the resonance condition of a sub-wavelength metal grating to the refractive index of the surrounding medium. We theoretically design a sub-wavelength Ag grating covered with a high-refractive-index medium layer and apply it to a ZnO ultraviolet photodetector. By optimizing the parameters (angle of incidence, grating period, grating spacing, grating thickness, high-refractive-index medium layer thickness, refractive index of the covering), the optical field is localized at the interface of the sub-wavelength Ag grating and the ZnO thin film; that is, surface plasmon resonance is realized within the device. Compared with the device without a high-refractive-index medium layer, the maximum absorption enhancement factor of the designed device can reach up to 108. This work will provide theoretical guidance to realize a surface plasmon resonance-enhanced ZnO ultraviolet photodetector with a sub-wavelength metal grating.

Key words: Surface plasmon resonance, sub-wavelength metal grating, ultraviolet photodetector, ZnO

INTRODUCTION

With the advantages of high saturation drift velocity, high radiation resistance and high breakdown voltage, zinc oxide (ZnO), a wide bandgap semiconductor, is considered to be an excellent material for ultraviolet detection.[1–5] At present, some progress has been achieved in the study on ZnO-based ultraviolet photodetectors. However, the low responsivity of ZnO ultraviolet photodetectors is the main factor that restricts their practical application.[6–10] It has been reported that the surface plasmon resonance effect of a sub-wavelength metal grating is an ideal way to improve the responsivity of a photodetector. When incident light with a suitable wavelength interacts with the sub-wavelength metal grating, surface plasmon resonance is induced and trapped at the metal–semiconductor interface. This results in an increased absorption in the semiconductor, which leads to a responsivity enhancement of the photodetector.[11–14] J. Hetterich et al. designed a photodetector based on a GaInNAs quantum well with a sub-wavelength Au grating.[12] With a grating periodicity of 820 nm and an electrode finger width of 460 nm, a 16-fold increase in

(Received December 14, 2019; accepted February 5, 2020; published online February 14, 2020)
Ji Yu and Hai-Jiao Men have contributed equally to this article.

the absorption was achieved compared with the case without the sub-wavelength Au grating. F. F. Ren et al. fabricated a photodetector based on Si with a sub-wavelength Al grating.[13] Due to the surface plasmon resonance effect, the photocurrent of the device was more than tripled. Q. Jing et al. also designed a photodetector based on Si with a sub-wavelength Al grating.[14] The absorption efficiency of the designed detector was 32% higher than that of a detector without the sub-wavelength metal grating. However, at present, the surface plasmon resonance effect of the sub-wavelength metal grating has been hard to realize in the ultraviolet region. First, this spectral region is close to the limit of the resonant frequency for the metals (e.g., Ag, Au and Al).[15] Second, the metal materials have a large absorption coefficient in the ultraviolet band, which leads to a large absorption loss.[16] Therefore, no suitable sub-wavelength metal grating structure has been found to improve the responsivity of a ZnO ultraviolet photodetector. It has been reported that the surface plasmon resonance condition of a sub-wavelength metal grating is sensitive to the refractive index of the surrounding medium. For example, W. Su et al. reported that the resonant angle changes with the refractive index of the media covering the Al grating.[17] Inspired by this, we designed a sub-wavelength Ag grating covered with a high-refractive-index medium layer, and applied the grating structure to a ZnO ultraviolet photodetector. The simulation results showed that the optical field is localized at the interface of the sub-wavelength Ag grating and the ZnO thin film; that is, the surface plasmon resonance effect of the sub-wavelength Ag grating is realized in the ultraviolet region. The optimal absorption enhancement factor of the device can reach up to 108. This work will provide theoretical guidance to realize a surface plasmon resonance-enhanced ZnO ultraviolet photodetector with a sub-wavelength metal grating.

STRUCTURE DESIGN AND SIMULATION SETUP

The device structure consisted of three separate parts, namely, (1) the high-refractive-index medium layer (covering), (2) the sub-wavelength Ag grating, and (3) the ZnO film (without considering its insulator substrate), as shown in Fig. 1. To induce surface plasmon resonance in the sub-wavelength Ag grating, a coupling mechanism was required to couple the incident radiation to the surface plasmon resonance modes, which can be described by the following equation:[17]

$$k_0 n_a \sin\theta_{\mathrm{R}} + m\frac{2\pi}{P} = \pm k_0 \sqrt{\frac{n_a^2 \varepsilon_m}{n_a^2 + \varepsilon_m}} \qquad (1)$$

where k_0 represents the free space wave vector, n_{a} is the refractive index of the medium which is in contacts with the surface of the grating, θ_{R} is the resonant angle of incidence, m is an integer, P is the grating period, the sign "+" corresponds to diffracted waves of orders $m > 0$ and sign "−" corresponds to diffracted waves of orders $m < 0$, and ε_{m} is the permittivity of the metal.

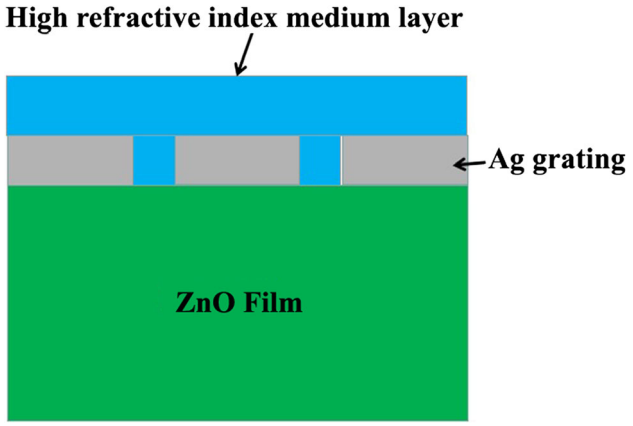

Fig. 1. Schematic diagram of a ZnO ultraviolet photodetector based on a sub-wavelength metal grating covered with a high-refractive-index medium.

The structure was simulated using the COMSOL Multiphysics software. In the simulation, the incident light wave was transverse-magnetic polarized. The refractive index of Ag and ZnO was provided by the software. The physical field in the simulation was the electromagnetic wave frequency domain of the radio frequency. Based on the simulation setup described above, parameters such as metal grating period, the incident angle of light, grating spacing, grating thickness, thickness of the high-refractive-index medium layer and the refractive index of the high-refractive-index medium layer were simulated, which will be discussed in the following section. The absorption enhancement factor is defined as the ratio of the normalized power transmittance of the designed structure to the normalized power transmittance of the structure without the high-refractive-index medium layer.

RESULTS AND DISCUSSION

In this section, we will discuss the effect of different parameters on the absorption enhancement factor of the device. In the entire simulation, the ZnO film thickness was kept at 750 nm, and the wavelength of incident light was set at 368 nm, which corresponds to the bandgap of ZnO at room temperature.[18] First, we studied the effect of the grating period and angle of incidence on the absorption enhancement factor. For a sub-wavelength metal grating, the grating period is less than the incident wavelength. So, for this simulation, the grating period was varied from 10 nm to 360 nm, and its step size was 10 nm. The angle of incidence was changed in the range of 0° to 90°, and its step size was 5°. The duty ratio was set as 0.5, and the grating thickness was kept constant at 100 nm. The refractive index and the thickness of the covering

were set as 2.8 and 150 nm, respectively. Through the simulation based on the above parameters, the maximum absorption enhancement factor of the device was 27 when the grating period was 210 nm and the angle of incidence was 55°, which is shown in Fig. 2.

Second, the effect of grating spacing on the absorption enhancement factor of the device was studied, which is shown in Fig. 3. The grating spacing was changed in the range of 10 nm to 200 nm, and its step size was 10 nm. The grating period was 210 nm, and the angle of incidence was 55°, which were obtained from the above simulation. Other parameters were set as: grating thickness was 100 nm, the refractive index of the covering was 2.8 and the thickness of the covering was 150 nm. As can be seen from the figure, when the grating spacing was less than 90 nm, the absorption enhancement factor of the device was very low and exhibited almost no change with a change in the grating spacing. When the grating spacing was more than 90 nm, the absorption enhancement factor of the device increased sharply and reached the maximum value (29) when the grating spacing was 100 nm, and then decreased with the increase of the grating spacing.

Third, the effect of the grating thickness on the absorption enhancement factor of the device is studied on the basis of the incident angle (55°), grating period (210 nm) and grating spacing (100 nm) determined from the above simulations, which are shown in Fig. 4. The grating thickness was changed in the range of 10 nm to 200 nm, and its step size was 10 nm. The refractive index of covering was 2.8 and the thickness of covering was 150 nm. Through the simulation based on the above parameters, the maximum absorption enhancement factor of the device was 93 when the grating thickness was 80 nm. It was obvious that the absorption enhancement factor significantly depends on the grating thickness of the device.

Fourth, based on the determination of the incident angle (55°), grating period (210 nm), grating spacing (100 nm) and grating thickness (80 nm), the effect of the high-refractive-index medium layer thickness on the absorption enhancement factor of the device was studied, which is shown in Fig. 5. The high-refractive-index medium thickness was

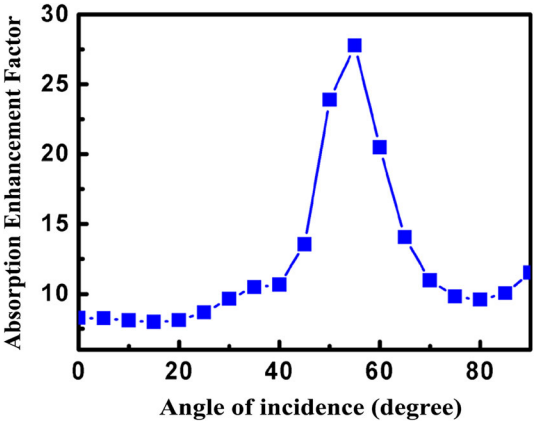

Fig. 2. Absorption enhancement spectrum for a grating period of 210 nm and an incident angle of 55°.

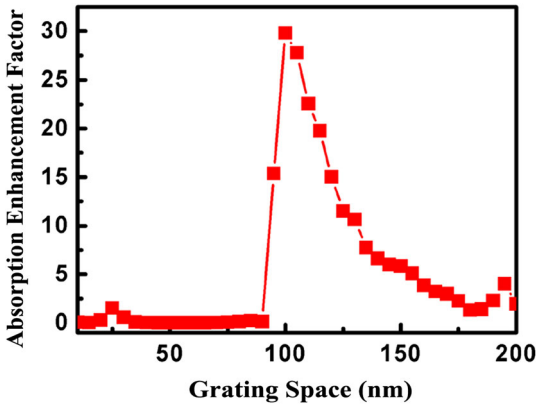

Fig. 3. Absorption enhancement spectrum for different grating spacings.

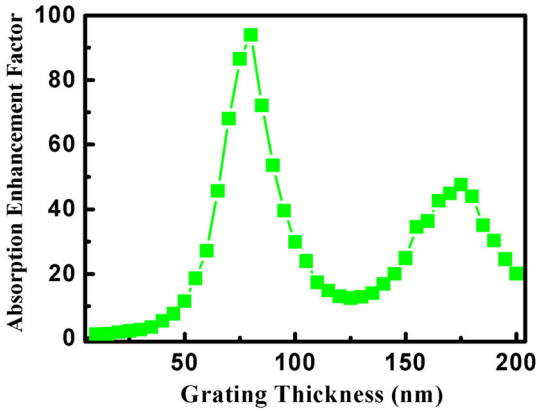

Fig. 4. Absorption enhancement spectrum for different grating thicknesses.

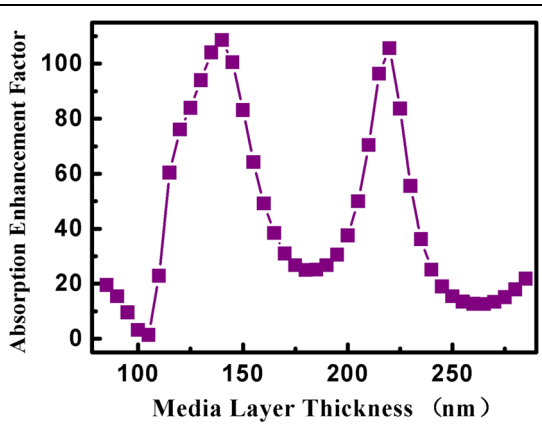

Fig. 5. Absorption enhancement spectrum for different high-refractive-index medium layer thicknesses.

changed in the range of 80 nm to 200 nm, and its step size was 10 nm. The refractive index of the covering was kept at 2.8. It was noted that the absorption enhancement factor of the device showed two extremes with the change of the high-refractive-index medium layer thickness, which may be related to the longitudinal Fabry–Perot resonance.[19] The maximum absorption enhancement factor of the device was 108 when the high-refractive-index medium layer thickness was 140 nm.

Fifth, based on an incident angle of 55°, grating period of 210 nm, grating spacing of 100 nm, grating thickness of 80 nm and high-refractive-index medium layer thickness of 140 nm, the effect of the refractive index of the covering on the absorption enhancement factor of the device was studied, which is shown in Fig. 6. The refractive index of the covering was changed from 2 to 3, and its step size was 0.2. According to the above parameters, the optimal refractive index of the covering was 2.8. Ultimately, through the simulation of the device, the following optimal parameters were determined: incident angle was 55°, grating period was 210 nm, grating spacing was 100 nm, grating thickness was 80 nm, high-refractive-index medium thickness was 140 nm and the refractive index of the covering was 2.8. The maximum absorption enhancement factor of the device based on the optimal parameters was 108. It can be seen that the refractive index of the coating had a great influence on the absorption enhancement factor of the device, which also proved that the surface plasmon resonance condition of the metal grating is sensitive to the refractive index of the surrounding medium. The material used as the coating not only requires a high refractive index but also needs to ensure that the incident 368-nm ultraviolet light is not absorbed. However, at present, we have not discovered a material that meets the above requirements.

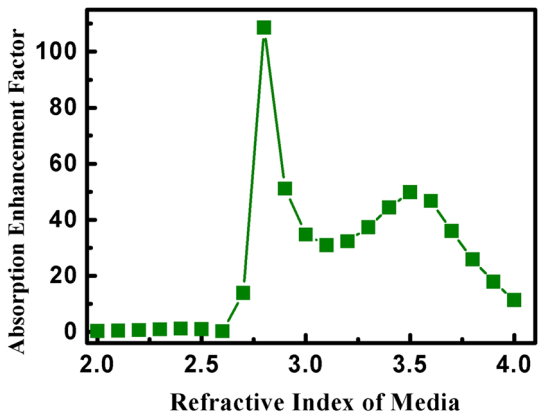

Fig. 6. Absorption enhancement spectrum for different refractive indexes of the covering.

Figure 7a and b shows the electric field distribution of the devices with and without the high-refractive-index medium layer, respectively. It should be noted that, based on the above optimum parameters, the electric field was located at the interface between the silver grating and ZnO film in the device covered with the high-refractive-index medium layer; that is, the surface plasmon resonance effect was realized in the designed structure.[20] In the uncovered device, the electric field was not located at the interface between the silver grating and the ZnO film, indicating that the surface plasmon resonance was not realized within the device.

CONCLUSIONS

In summary, we have designed a ZnO ultraviolet photodetector with a sub-wavelength Ag grating covered with a high-refractive-index medium layer. By optimizing the device parameters, the surface plasmon resonance effect is successfully realized in the device. Compared with a device without the high-refractive-index medium layer, the maximum absorption enhancement factor of the designed device can reach up to 108. The results obtained in this study can be used as a reference for the

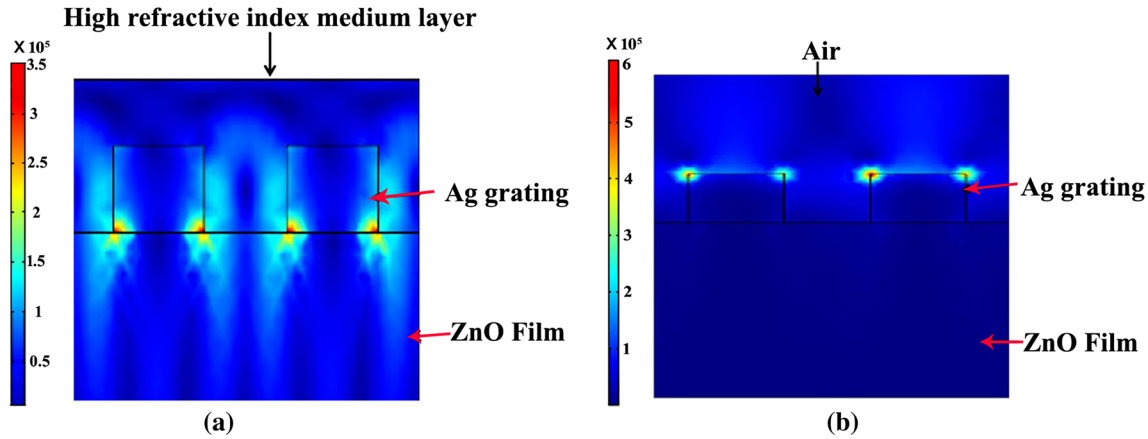

Fig. 7. Electric field distribution of the devices based on parameters obtained from the above simulation: (a) with the high-refractive-index medium layer; (b) without the high-refractive-index medium layer.

research of surface plasmon resonance-enhanced ultraviolet photodetectors based on a sub-wavelength metal grating.

ACKNOWLEDGMENTS

This work is supported by the National Natural Science Foundation of China (no. 11804235) and the Major Incubation Project of Shenyang Normal University (51700303). We thank Liwen Bianji, Edanz Group China (www.liwenbianji.cn/ac), for editing the English text of a draft of this manuscript.

REFERENCES

1. K.W. Liu, M. Sakurai, and M. Aono, *Sensors* 10, 8604 (2010).
2. J. Yu, C.X. Shan, Q. Qiao, X.H. Xie, S.P. Wang, Z.Z. Zhang, and D.Z. Shen, *Sensors* 12, 1280 (2012).
3. H.Y. Chen, K.W. Liu, X. Chen, Z.Z. Zhang, M.M. Fan, M.M. Jiang, X.H. Xie, H.F. Zhao, and D.Z. Shen, *J. Mater. Chem. C* 2, 9689 (2014).
4. P.N. Ni, C.X. Shan, S.P. Wang, B.H. Li, Z.Z. Zhang, D.X. Zhao, L. Liu, and D.Z. Shen, *J. Phys. Chem. C* 116, 1350 (2012).
5. P.N. Ni, C.X. Shan, S.P. Wang, X.Y. Liu, and D.Z. Shen, *J. Mater. Chem. C* 1, 4445 (2013).
6. H.Y. Chen, H. Liu, Z.M. Zhang, K. Hu, and X.S. Fang, *Adv. Mater.* 28, 403 (2016).
7. K.W. Liu, M. Sakurai, M.Y. Liao, and M. Aono, *J. Phys. Chem. C* 114, 19835 (2010).
8. J. Yu, C.X. Shan, X.M. Huang, X.W. Zhang, S.P. Wang, and D.Z. Shen, *J. Phys. D Appl. Phys.* 46, 305105 (2013).
9. J.S. Liu, C.X. Shan, B.H. Li, Z.Z. Zhang, C.L. Yang, D.Z. Shen, and X.W. Fan, *Appl. Phys. Lett.* 97, 251102 (2010).
10. J. Yu and N. Tian, *Phys. Chem. Chem. Phys.* 18, 24129 (2016).
11. H.Y. Chen, L.X. Su, M.M. Jiang, and X.S. Fang, *Adv. Funct. Mater.* 27, 1704181 (2017).
12. J. Hetterich, G. Bastian, N.A. Gippius, S.G. Tikhodeev, G.V. Plessen, and U. Lemmer, *IEEE. J. Quantum. Elect.* 43, 855 (2007).
13. F.F. Ren, K.W. Ang, J.F. Song, Q. Fang, and M.B. Yu, *Appl. Phys. Lett.* 97, 091102 (2010).
14. J. Qiao, S. Xie, L.H. Mao, J. Cong, and W.F. Dong, *Chin. J. Lumin.* 39, 363 (2018).
15. H.Y. Chen, K.W. Liu, M.M. Jiang, Z.Z. Zhang, L. Liu, B.H. Li, X.H. Xie, F. Wang, D.X. Zhao, C.X. Shan, and D.Z. Shen, *J. Phys. Chem. C* 118, 679 (2014).
16. H.Y. Chen, K.W. Liu, M.M. Jiang, Z.Z. Zhang, X.H. Xie, D.K. Wang, L. Liu, B.H. Li, D.X. Zhao, C.X. Shan, and D.Z. Shen, *Appl. Phys. Lett.* 104, 091119 (2014).
17. W. Su, G.G. Zheng, and X.Y. Li, *Opt. Commun.* 285, 4603 (2012).
18. J.H. Lin, Y.J. Chen, H.Y. Lin, and W.F. Hsieh, *J. Appl. Phys.* 97, 033526 (2005).
19. F.F. Masouleh, N. Das, and H.R. Mashayekhi, *Opt. Quant. Electron.* 47, 193 (2015).
20. C.L. Tan, V.V. Lysak, K. Alameh, and Y.T. Lee, *Opt. Commun.* 283, 1763 (2010).